Int. J. Electrochem. Sci., 9 **(2014)** 1964 - 1985

International Journal of
ELECTROCHEMICAL
SCIENCE
www.electrochemsci.org

Electrochemical Investigation of Green Inhibitor Adsorption on Low-Carbon Steel in Produced Water

M.A. Ameer[*]*, A.M. Fekry and A.Othman*

Chemistry Department, Faculty of Science, Cairo University, Giza-12613, Egypt.
[*]E-mail: mameer_eg@yahoo.com

Received: 10 October 2013 / *Accepted:* 8 December 2013 / *Published:* 1 April 2014

The electrochemical behavior of low carbon steel in produced water containing different concentrations of ascorbic acid (AA) has been studied by potentiodynamic polarization, electrochemical impedance spectroscopy (EIS) measurements and confirmed by surface examination via scanning electron microscope (SEM). The results of EIS and polarization data showed that the corrosion rate of the steel decreases by increasing both the concentration of AA (0.01-0.1M) and temperature under study (303-333K). The maximum efficiency was obtained (88%) in 0.1M AA at 333K. Thermodynamic parameters indicate that the adsorption of AA on low carbon steel followed both physical as well as chemical adsorption mechanisms.

Keywords: Low carbon steel; Produced water; Green inhibitor adsorption; EIS; Potentiodynamic; SEM.

1. INTRODUCTION

The extent of low carbon steel corrosion problems in the oil industries depends on the fluid composition such as oil type, oil to water ratio, and water salinity. The role of water, dissolved oxygen, CO_2, H_2S, dissolved salts, pH, temperature and velocity on corrosion control of steel in oil fields has been discussed and addressed by several authors[1-3]. The use of corrosion inhibitors in petroleum production is essential for corrosion control in these corrosive environments [4,5]. Produced water is characterized with high chloride ion content which plays a big role in the corrosion process of structural steel, since in environments containing high concentrations of chloride ions, β-FeOOH unquestionable exists, as the concentration of Cl^- ions increased, the content of β-FeOOH increased in the rust phase. The water salinity affects the solubility of gases that have a great influence on the corrosivity of the environment. The presence of sodium chloride in concentrations of up to 1 wt%

increases the corrosion rate, because it prevents the formation of a protective FeS film on the low carbon steel surface [2].

From the foregoing, it is obvious that chloride ions actually influence the corrosion behavior, as well as the morphology. Moreover β-FeOOH formed on steel surface at high chloride ion concentration promotes the corrosion process.

Among alternative corrosion inhibitors, organic products containing one or more polar functions (with N, O and S atoms) and π-electrons have shown to be quite efficient to prevent corrosion [6,7]. Adsorption of such inhibitors on the carbon steel surface represents the most important action of these compounds. The extent and mode of adsorption depends on definite physico-chemical properties of the organic molecule, such as functional groups, aromaticity and π orbital character of the donating electrons steric effects, and electron density of the donor atom and the electronic structure of the molecule [8]. The adsorption extent also depends on the nature of the metal surface and the electrolyte. Adsorption results in an effective blocking of the active sites of metal dissolution and/or hydrogen evolution, thus diminishing the overall corrosion rate.

One way of protecting carbon steel from corrosion is to use corrosion inhibitors [9-14]. Application of small biomolecules such as ascorbic acid (AA) as environmental-friendly,

low-cost, readily available corrosion inhibitors of rebar corrosion would be favorable. AA has already been proved as a good steel corrosion inhibitor in acidic [15,16], neutral media [17,18] and alkaline media [19]. The AA effect on the corrosion of mild steel in pH 2 – 6 solutions was investigated by *Ferreira* et al.[15]. *Goncalves* et al [16] have found that the presence of AA decreases the anodic current values of steel in 0.5 mol dm^{-3} Na_2SO_4 at pH 2.7, and have related the effect to the adsorption of AA at the active sites of the electrode surface and blocking of the water adsorption reaction that is involved in the oxide layer formation.

The used ascorbic acid inhibitor ($C_6H_8O_6$) in such investigation is a naturally occurring organic compound with antioxidant properties. It is a white solid, but impure samples can appear yellowish. It dissolves well in water to give mildly acidic solutions. AA resembles the sugar from which it is derived, being a ring containing many oxygen-containing functional groups. The molecule exists in equilibrium with two ketone tautomers, which are less stable than the enol form. The inhibition impact of ascorbic acid is usually attributed to interactions with metallic surfaces by adsorption. The polar function is frequently regarded as the reaction center for the adsorption process establishment being the adsorption bond strength determined by the electron density and polarizability of the functional group[20].

The aim of this study is to investigate the efficiency of ascorbic acid (AA) for the corrosion inhibition of low carbon steel in produced water using impedance and potentiodynamic techniques. The effects of inhibitor concentration and temperature on the performance and extent of adsorption of inhibitor are studied.

2. EXPERIMENTAL

The working electrode with a fixed surface area of 1 cm^2 was made from low carbon steel specimen. The chemical compositions of the low carbon steel(St. 37) studied (wt. %) is: 0.07C, 0.07Si,

0.063Mn, 0.004P, 0.002S, 0.01 Cr, 0.003Mo, 0.01Ni, 0.04Al, 0.03Cu, 0.002V and the rest is Fe. The surface of the test electrode was mechanically polished by emery papers to ensure the same surface roughness and obtain a mirror like finish. A typical three-electrode cell was used fitted with a large platinum sheet of size 15*20*2 mm as counter electrode and saturated calomel (SCE) reference electrode (E_{SCE} =0.241 V). The test solution used was produced water (blank) associated crude oil (pH = 5.8). The analysis of the formation water has been carried out using ionic chromatograph instrument and its chemical composition (ppm) is : 133207Cl^-, 22400TDS, 8400 $Ca^{2+}$and 3395 Mg^{2+}. Ascorbic acid ($C_6H_8O_6$) was obtained from (Aldrich) analytical reagent. Electrochemical impedance spectroscopy (EIS) was recorded with an excitation of ac signal of 10 mV peak to peak in a frequency domain from 100 kHz down to 100 MHz. The instrument used is a workstation IM6e (Zahner-elektrik, GmbH, Kronach, Germany). Cathodic and anodic polarization curves were traced at a scan rate of 1 m V s^{-1}. The SEM micrographs were collected using a JEOL JXA-840A electron probe microanalyzer.

3. RESULTS AND DISCUSSION

3.1. EIS measurements

3.1.1. Effect of ascorbic acid concentration

Table 1. Kinetic parameters derived from EIS plots of low carbon steel in produced water in (a) absence and (b) presence of AA at different temperatures after immersion for 60 min.

(a)

Temperature (K)	R_1 (Ω cm^2)	C_1 (μ F cm^{-2})	α_1	R_2 (Ω cm^2)	C_2 (μ F cm^{-2})	α_2	R_s (Ω cm^2)	C_T^{-1} (μ F^{-1} cm^2)*10^3
303	6.65	176.2	0.83	131.7	617.7	0.64	2.095	7.2943
313	3.94	157.0	0.92	128.2	488.2	0.58	2.099	8.4178
323	5.68	879.4	0.51	29.79	219.5	0.94	1.715	5.6929
333	1.99	1151.0	0.53	15.41	370.5	0.86	1.717	3.5679

(b)

Temperature (K)	Concn. (M)	R_1 (Ω cm^2)	C_1 (μ F cm^{-2})	α_1	W (Ω cm^2 $S^{-1/2}$)	C_2 (μ F cm^{-2})	α_2	R_s (Ω cm^2)	C_T^{-1} (μ F^{-1} cm^2)*10^3
303	0.10	50.41	138.9	0.54	914.3	52.41	0.75	1.59	26.27
	0.07	20.07	83.56	0.49	622.1	79.2	0.67	2.27	24.59
	0.05	17.3	185.4	0.49	577.1	67.9	0.71	2.09	20.12
	0.01	14.01	143.6	0.50	271.3	81.37	0.74	1.84	19.25
313	0.10	110.8	101	0.46	809	194.8	0.81	0.95	15.03
	0.07	215	230	0.60	528.56	95.09	0.72	0.70	14.86
	0.05	180	251.7	0.68	426.26	121.4	0.79	1.01	12.21
	0.01	112.8	188.1	0.56	230	189.3	0.69	1.10	10.59
323	0.10	117.1	96.7	0.56	650	163.7	0.82	1.5	16.45
	0.07	190	155.9	0.49	407.21	151.8	0.85	0.73	13.00
	0.05	115	134.3	0.61	318.94	174.0	0.68	0.79	13.19
	0.01	109	457.2	0.49	183.79	127.8	0.67	1.45	10.01

333	0.10	105	158. 4	0.56	429.23	119.5	0.81	1.45	14.65
	0.07	130	195.4	0.55	325.5	137	0.81	0.97	12.47
	0.05	92	310.8	0.62	242.13	166.4	0.74	0.95	9.23
	0.01	95	548.9	0.49	154.8	154.1	0.72	1.30	8.31

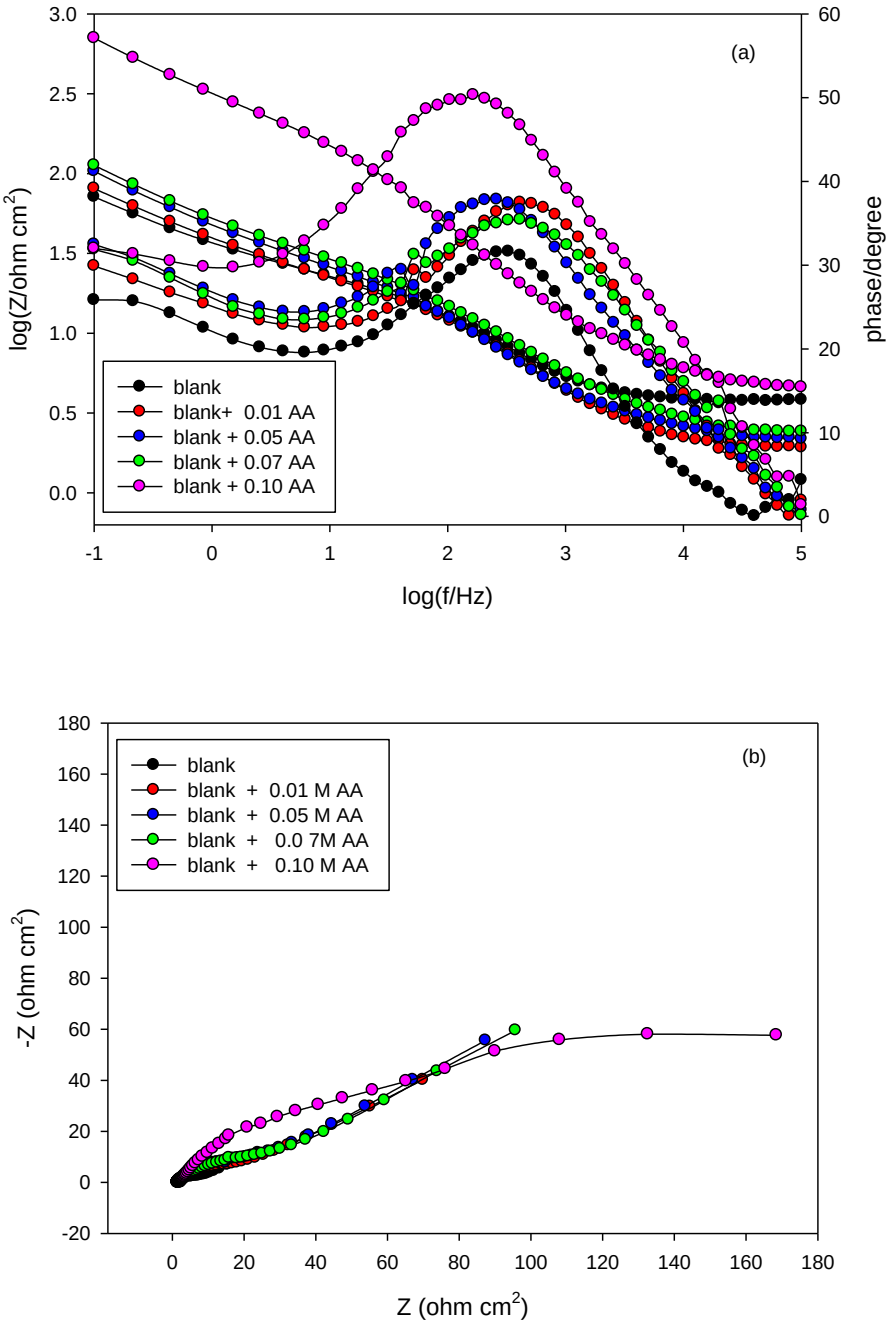

Figure 1. (a) Bode and (b) Nyquist plots of low carbon steel electrode in produced water (blank) without and with different concentrations of AA at 303K

The EIS scans of low carbon steel in dependence on the concentration of ascorbic acid inhibitor were recorded after the working electrode was left in the test solution for 60 minutes to achieve its

steady free corrosion potential (E_{st}). The experimental EIS measurements are presented as Bode and Nyquist plots in Fig. 1a & b, respectively. The impedance |Z| of low carbon steel alloy is clearly found to depend on the inhibitor concentration (0.01,0.05, 0.07 and 0.1M). An increase in inhibitor concentration leads to an increase in the |Z| value. The results in presence of AA, show two time constants, one of them has phase angle maximum ~ 45º, corresponding to a diffusion control in the passive layer.

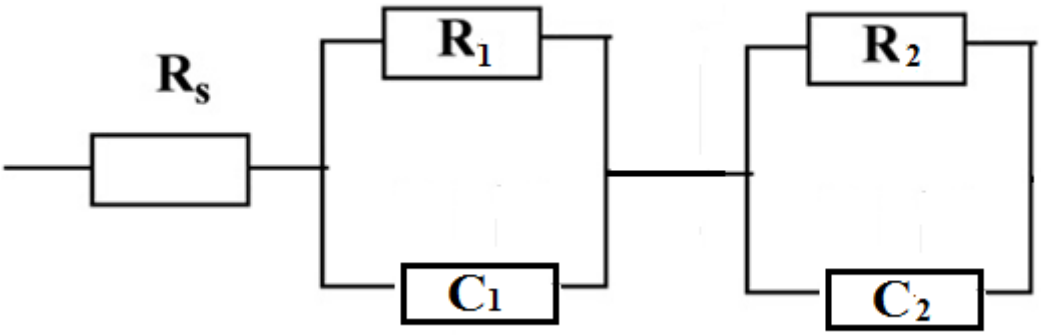

(a)

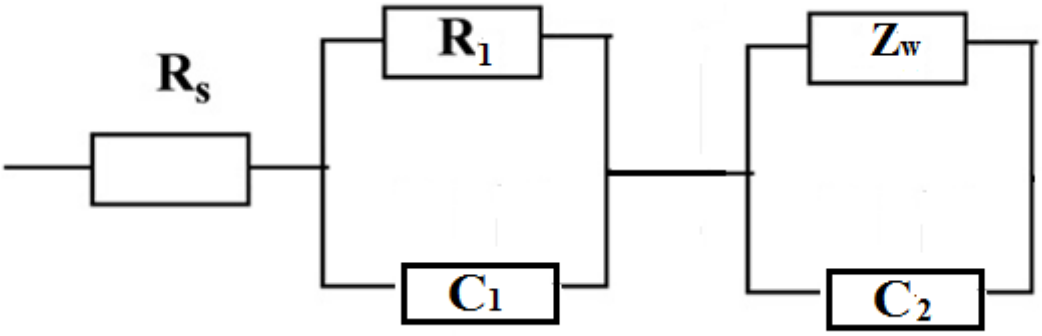

(b)

Figure 2. (a) Equivalent circuit model for EIS tests in blank without and (b) with addition of AA

The impedance data were thus simulated to the appropriate equivalent circuits (Fig. 2a&b). The data for blank solution (produced water without AA) shows two time constants with equivalent circuit shown in Fig. 2a. This simulation gave a reasonable fit with an average error of about 3%. The estimated data is given in Table 1a&b for blank without and with different concentrations of AA, respectively. The appropriate equivalent model used to fit the high and low frequency data consists of two circuits in series from $R_1Z_wC_1$ and R_2C_2 parallel combination and the two are in series with R_s (Fig.2b). In this way C_1 is related to contribution from the capacitance of the outer layer and the faradaic reaction therein and C_2 pertains to the inner layer, while R_1 and R_2 are the respective resistances of the outer and inner layers constituting the surface film, respectively [21]. One of the

peaks in Bode plots has phase angle maximum ~ 45, thereby an equivalent circuit with Warburg component Z_w might be more appropriate. A Warburg impedance (Z_w) can be linked to ion diffusion through the passive film. Such diffusion process may indicate that the corrosion mechanism is controlled not only by a charge-transfer process but also by a diffusion process. Analysis of the experimental spectra was made by best fitting to the corresponding equivalent circuit using Thales software provided with the workstation where the dispersion formula suitable to each model was used [22].

In this complex formula an empirical exponent (α) varying between 0 and 1, is introduced

to account for the deviation from the ideal capacitive behavior due to surface inhomogeneities, roughness factors and adsorption effects [23]. An ideal capacitor corresponds with α= 1 while α= 0.5 becomes the CPE in a Warburg component [24]. In all cases, good conformity between theoretical and experimental was obtained for the whole frequency range with an average error of 3%.

As given in Table 1b, the relative thickness ($1/C_T = 1/C_1 + 1/C_2$) of the surface film on low carbon steel sample increases with increasing inhibitor concentration in produced water and also the diffusion behavior increases (Warburg impedance value). Thus, when inhibitor concentration increases, more inhibitor molecules will be adsorbed on the surface through the active centers in AA compound which may be double bonds or hetero atoms like oxygen.

It is known that AA is unstable when present in a solution at pH higher than 4[25]. AA, being a weak organic acid, is readily doubly deprotonated forming the ascorbate anion. Since ascorbate anion is unstable and easily-oxidizable, it is expected to be rapidly air-oxidized to dehydro-ascorbic acid (DAA) and eventually to 2,3-diketogluconic acid (DGA) [26]. The final products of further decomposition are threonic (TA) and oxalic acid (OXA) as shown in following reactions:

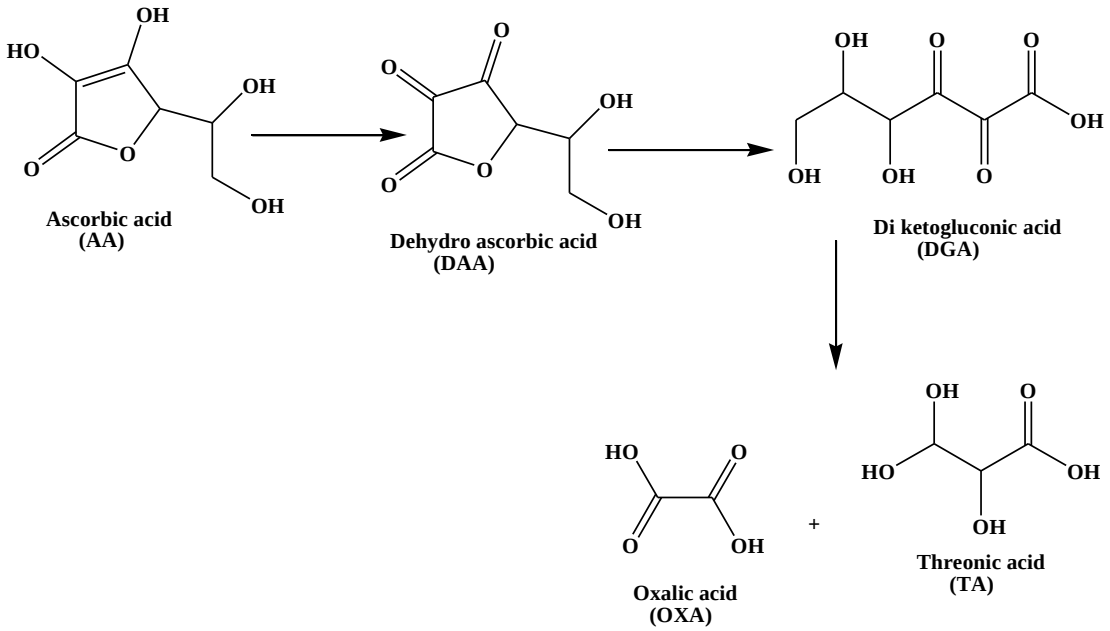

AA is present as an undissociated molecule and incapable of reducing DAA. This has been explained by the chemical characteristics and structures of the molecules involved. It has been demonstrated, by the molecular orbital method, that the elements of the molecular structure of AA anion are very similar to the monocyclic tri-ketone structure of the DAA [26]. Considering the great electron donating ability of the AA anion, it is reasonable to assume that it would reduce DAA more

easily than undissociated AA. Moreover, interconversion between AA and DAA would preserve these compounds form oxidative decomposition allowing them to adsorb at the metal surface. This assumption is partly corroborated by the comparison of the AA and OXA inhibitive action and OXA showing considerably lower corrosion inhibition efficiency than AA. Because of its known electron donating ability as well as the Fe(II) and Fe(III) chelating properties[27]. AA anion would be the most probable adsorbing species in the investigated system.

3.1.2. Effect of temperature

The effect of temperature on the inhibition efficiency was determined for low carbon steel in produced water containing different concentration of ascorbic acid (0.01-0.1) at different temperatures ranging from 303 to 333 K. The results are given in Table 1a&b for blank (produced water) without and with ascorbic acid, respectively. The inhibition efficiencies of AA were found to increase with increasing temperature from 303 to 333 K. Such inhibitor is of practical interest where retardation of corrosion at elevated temperatures is desired. Such result was observed for some Schiff bases inhibitor[28].

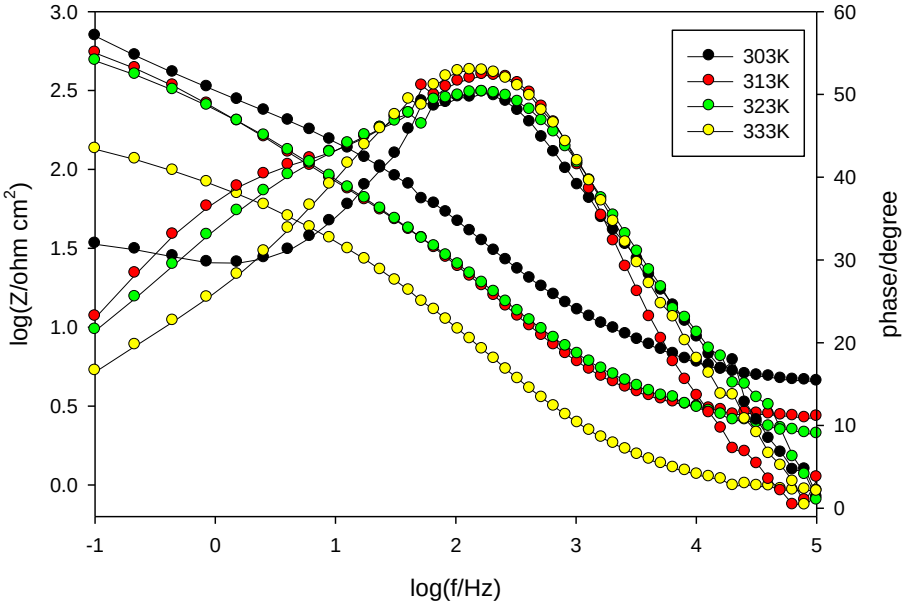

Figure 3. Bode plots of low carbon steel electrode in produced water (blank) with 0.1M AA at different temperatures.

Fig.3 represents Bode plots of low carbon steel electrode in produced water (blank) with 0.1M AA at different temperatures The plots are best fitted to the same model for the blank and the inhibited low carbon steel. The estimated parameters are given in Table 1a&b for the blank and the inhibited low carbon steel, respectively. It was found that both of R and W values decrease with increasing temperature. This suggests that higher temperatures can preclude film growth process as the alloy undergoes passivity breakdown due to enhanced solubility of the corrosion products, leading to a significant decrease in surface film stability. Moreover, one can suppose that at temperatures

corresponding to the equilibrium conditions, most of the surface film dissolves into the medium during the immersion period (60 min) leaving a quite thin barrier layer with lower corrosion resistance, which can sustain an electric field across the interface. Also, Warburg impedance values decrease with increasing temperature.

Fig.3 shows Bode plots for low carbon steel in blank with 0.1M concentration of AA at different temperatures. The plots are best fitted to the same model shown in Fig. 3b . The estimated parameters are given in Table 1a& b for the blank and the inhibited steel, respectively. It was found that R, W values or phase angle maximum decrease with increasing temperature. Rather, the relative film thickness ($1/C_T$) coincide well with this behavior.

3.2. Potentiodynamic polarization measurements

3.2.1. Effect of inhibitor concentration

In this part the potentiodynamic polarization behavior of low carbon steel was studied in relation to inhibitor concentration(0.01-0.1M).The potential was scanned automatically from -1.0 to 0.0 V vs. SCE at a rate of 1 mVs^{-1} which allows the quasi-stationary state measurements. Prior to the potential scan the electrode was left under open-circuit conditions in the respective solution for 60 min.until a steady free corrosion potential (E_{st}) value was recorded.

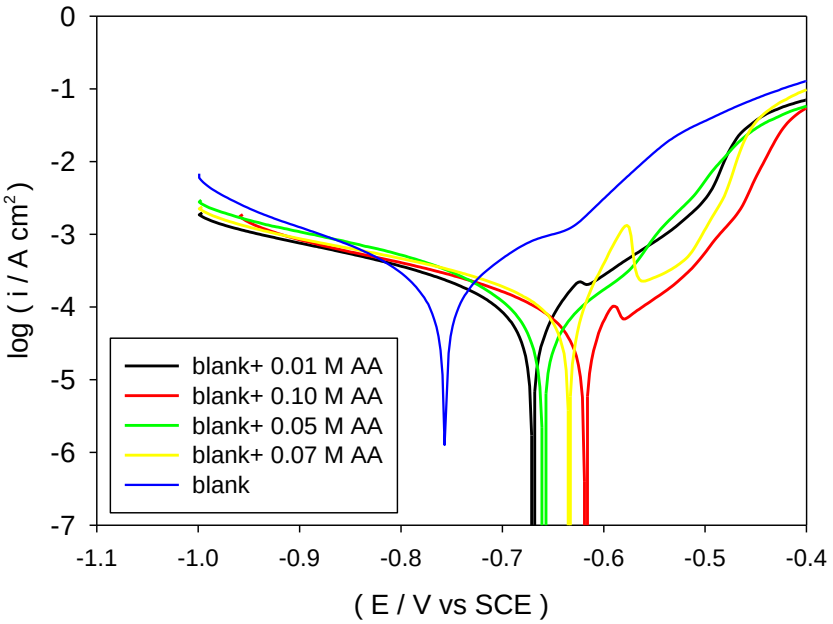

Figure 4. Polarization scans of low carbon steel electrode in produced water (blank) without and with different concentrations of AA at 303K

Fig.4 shows linear sweep potentiodynamic traces for the steel in blank containing different concentrations of AA at 303. It is noticed that the corrosion potential shifts towards more positive potential as the inhibitor concentration increases, indicating that these inhibitor promotes passivation

of steel through adsorption . This also can be attributed to deposition of the inhibitor molecules on the alloy as a result of interaction between the inhibitor and the metal surface that can effectively seals the surface against further reaction. It can be also concluded that the anodic process predominates over the cathodic ones.

Table 2. Kinetic parameters derived from Tafel plots of low carbon steel in produced water in presence and absence of different concentration of AA at different temperatures.

Temp. (K)	Conc. (M)	β_c (mV/dec)	β_a (mV/dec)	$i_{corr.}$ ($\mu A\ cm^{-2}$)	ρ ($g\ m^{-2}\ day^{-1}$)	E_{corr} (mV)	IE%
303	0.10	-62.1	88.6	23.0	5.7270	-709.8	84
	0.07	-99.9	186	37.6	9.3624	-721.5	75
	0.05	-68.0	111	56.2	13.9938	-747.2	63
	0.01	-133.0	169	80.0	19.9200	-741.5	47
	0.00	-155	130	143.8	35.8062	-757.3	--
313	0.10	-78.1	85.2	38.3	9.5367	-706.6	80
	0.07	-132.0	34.6	55.2	13.7448	-718.8	72
	0.05	-118.0	29.7	76.4	19.0236	-728.5	61
	0.01	-186.0	110.0	101.0	25.1490	-733.6	48
	0.00	-190	113.0	191.5	47.6835	-745.5	--
323	0.10	-108.0	89.8	49.2	12.2508	-652.2	87
	0.07	-77.7	49.9	70.1	17.4549	-654.9	81
	0.05	-56.1	48.8	99.1	24.6759	-672.3	74
	0.01	-154.0	117.0	127.2	31.6728	-697.6	67
	0.00	-170.0	112.0	378.5	94.2465	-822.8	--
333	0.10	-66.4	117	68.8	17.1312	-689.6	88
	0.07	-66.2	115	102.0	25.3980	-675.7	80
	0.05	-82.9	29	148.2	36.9018	-664.9	70
	0.01	-110.0	157	219.6	54.6804	-761.6	56
	0.00	-146.0	113	573.3	142.7517	-812.4	--

For all tested concentrations, the active dissolution parameters including the values of the corrosion potential (E_{corr}) and corrosion current density (i_{corr}) are given in Table 2 for both uninhibited and inhibited low carbon steel. It can be seen from the experimental results derived from polarization curves that increasing AA inhibitor concentration decreased i_{corr} significantly at all studied concentrations. A positive shift in corrosion potential was observed. The shift in corrosion potential towards the anodic side indicates that AA inhibitor is an efficient anodic inhibitor for low carbon steel in produced water. The inhibition efficiency can be calculated from the following equation[29]:

$$\%IE = (1 - \frac{i_{inh}}{i_{corr}})\ 100 \qquad (1)$$

where i_{corr} and i_{inh} are the corrosion current densities in absence and presence of AA, respectively. The data in Table 2 show that inhibition efficiency increases with increasing the concentration of AA. The increase in efficiency may be due to the blocking effect of the surface by both adsorption and film formation mechanism which decreases the effective area of attack. Results of

the inhibition efficiencies revealed the good inhibiting action of AA at high concentrations reaching the maximum value, 84%, at 0.1M at 303 K. The decrease of the corresponding current densities with increasing the inhibitor concentration was the consequence of the inhibitor adsorption on the steel surface.

3.2.2. Effect of temperature

To evaluate the adsorption of AA inhibitor at different concentrations and activation parameters of the corrosion processes of steel polarization parameters are investigated in the absence and presence of inhibitor at temperature range of 303 to 333 K and presented in Table 2. Fig.5, is an example of potentiodynamic polarization of low carbon steelin different concentration of AA at 333K. Fig. 6 shows the relation between log corrosion current density and the inhibitor concentration at different temperatures.

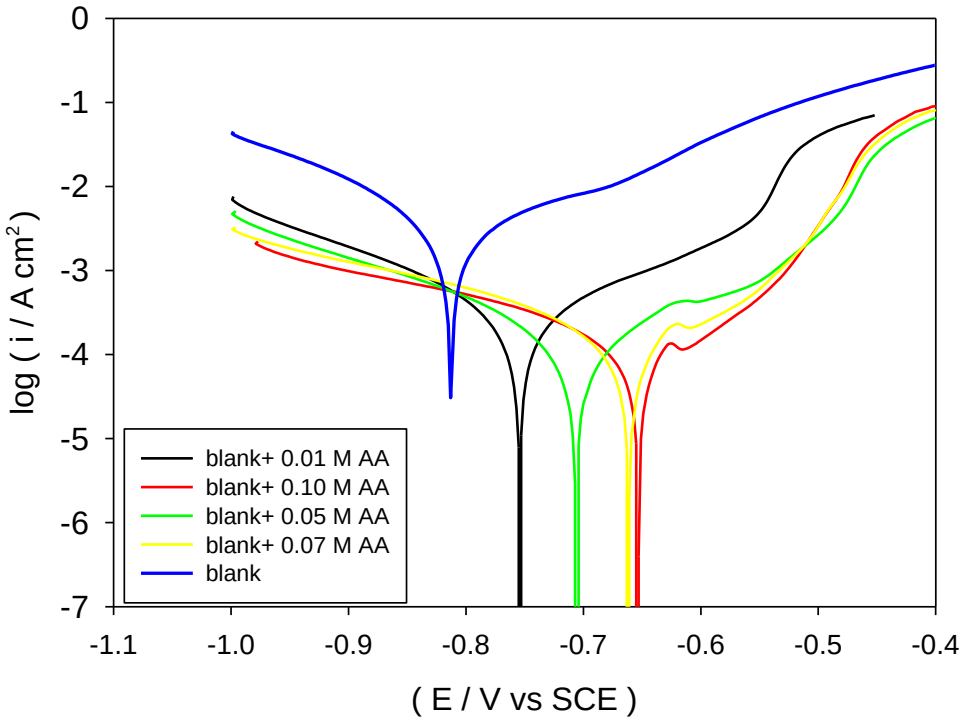

Figure 5. Polarization scans of low carbon steel electrode in produced water (blank) without and with different concentrations of AA at 333K

The values of i_{corr} increase with temperature indicating activation in the dissolution process of the surface oxide film associated with a reduction in its protective properties. This behavior may be attributed to some intrinsic modifications made by the film in its chemical composition and/or physical structure. The corrosion rate can be calculated from the relation(ρ):1 mA cm^{-2} = (8.95 M/n) g m^{-2} day^{-1}. For example, if the metal is steel (Fe), the number of electrons, n =2, atomic mass, M = 55.85 g and

density, d = 7.88 g cm^{-3} and the conversion becomes:1 mA cm^{-2} = 11.6 mm y^{-1} = 456 mpy = 249 g m^{-2} day^{-1}

It can be seen that the rise of temperature leads to an increase in corrosion rate in the absence and presence of inhibitor. The corrosiveness is significantly limited in the presence of inhibitor concentration and it can be seen that the corrosion current density for steel increases to a large extend with temperature in uninhibited solution than in inhibited one.

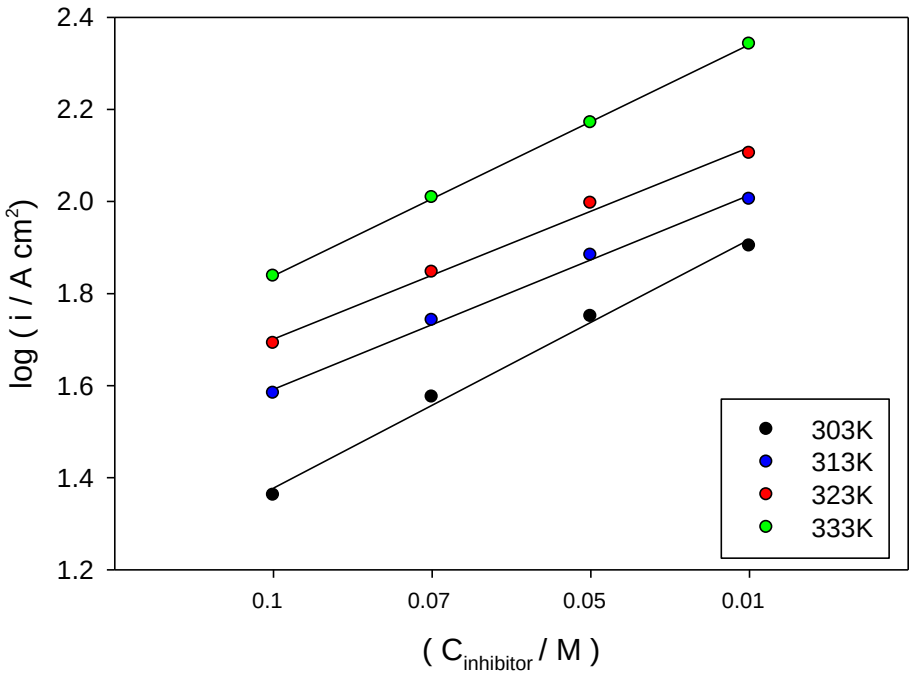

Figure 6. Variation of log i_{corr} with AA concentration for low carbon steel at different temperatures

This result confirms that AA decreases the corrosion process by acting as an efficient corrosion inhibitor with maximum inhibition efficiency at 333K(88%).Thus,

lowering corrosion action is enhanced more at higher temperatures compared to lower ones.

The apparent activation energy, E_a, of the corrosion reaction was determined using Arrhenius plots. Arrhenius equation could be written as:

$$\log i_{corr} = \log A - E_a / 2.303RT \qquad (2)$$

where i_{corr} is the corrosion current density, E_a the apparent activation factor. The apparent activation energy of the corrosion reaction in the presence and absence of the inhibitor could be determined by plotting log i_{corr} against 1/T which gives a straight line with a slope permitting the determination of E_a as shown in Fig. 7.

The linear plots show that at any temperature the rate of corrosion for uninhibited low carbon steel is higher than that for the inhibited one. The calculated values of the apparent activation corrosion energies in the absence and presence of different inhibitor concentration are listed in Table 3.

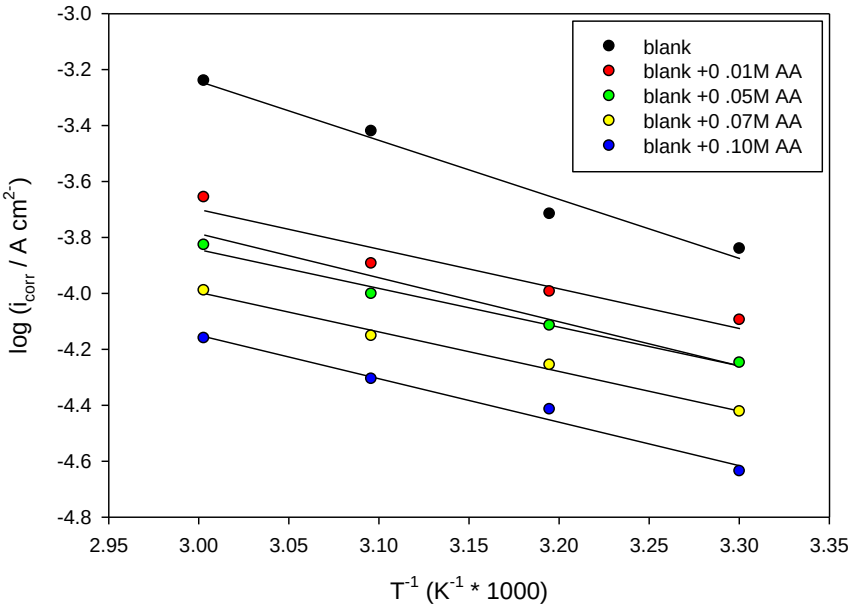

Figure 7. Variation of log i_{corr} with T^{-1} for low carbon steel in produced water (blank) without and with different concentration of AA at 303K

Table 3. Binding constant, number of active sites values obtained from Langmuir, the Kinetic-Thermodynamic , Flory-Huggins and Dubinin–Radushkevich (DRIM) isotherm models for AA at different temperature

Temp. (K)	Langmuir		Kinetic-thermodynamic			Flory-Huggins			DRIM		
	K_{ads}	R^2	1/y	K_{ads}	R^2	x	R^2	-a	θ_{max}	E_t	R^2
303	93.2	0.9973	1.3543	93.1	0.9871	1.4852	0.9725	0.0127	1.014	6.28	0.9958
313	64.7	0.9928	1.2666	65.2	0.9687	1.3156	0.9256	0.0141	1.015	5.95	0.9941
323	57.6	0.9869	1.2721	57.8	0.9565	1.2969	0.8951	0.0138	1.009	6.01	0.9886
333	54.4	0.9861	1.4016	49.3	0.9644	1.5519	0.9084	0.0130	0.984	6.21	0.9821

A decrease in inhibition efficiency with rise in temperature, with analogous increase in corrosion activation energy in the presence of inhibitor compared to its absence, is frequently interpreted as being suggestive of formation of an adsorption film of physical (electrostatic) nature. The effect, corresponding to an increase in inhibition efficiency with rise in temperature and lower activation energy in the presence of inhibitor, suggests a chemisorption mechanism [30,31].

From the foregoing, the trend for AA in produced water suggests a predominant effect followed both physical as well as chemical adsorption mechanism.

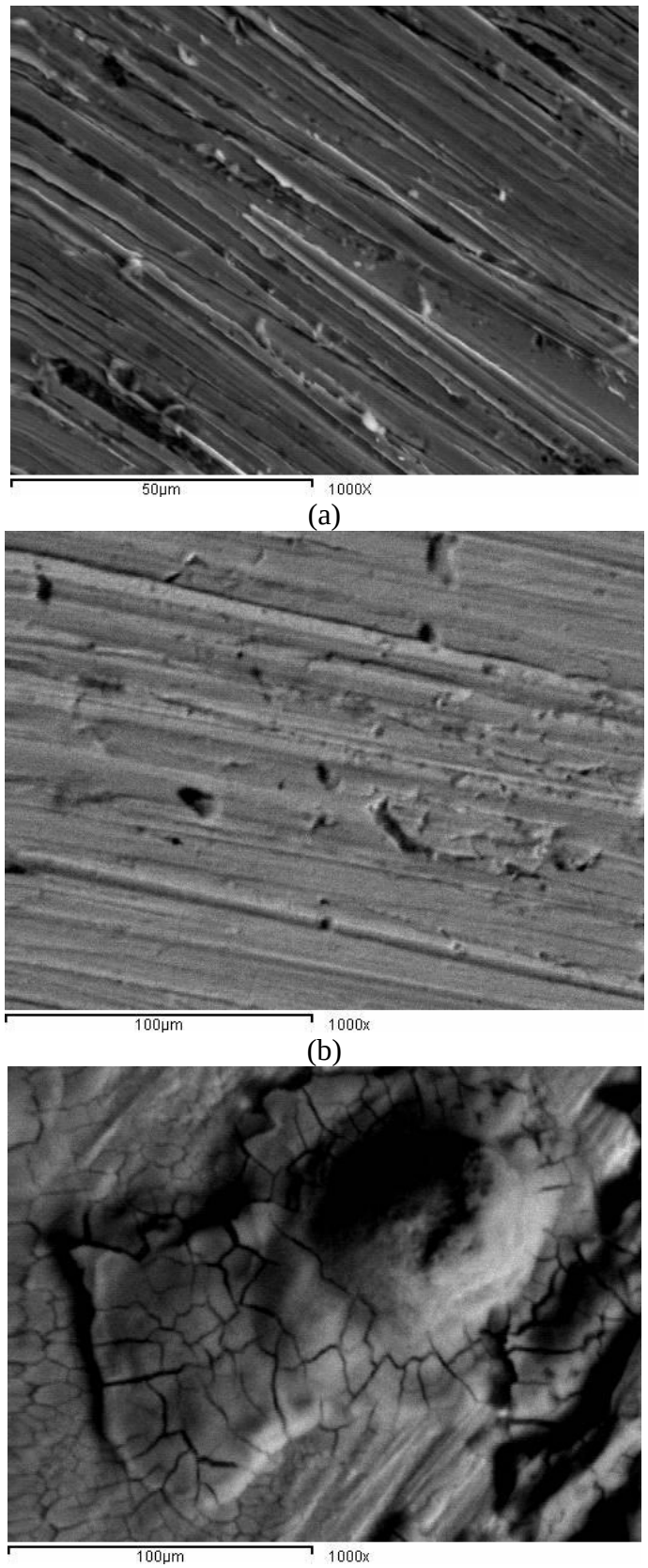

Figure 8. SEM images of low carbon steel after exposure in produced water (blank) containing various concentrations of AA for 60 min at 303K (a) blank, (b) 0.01M AA, (c) 0.1M AA

Scanning electron microscope (SEM) images were shown in Fig.8a–c for low carbon steel in blank without and with 0.01 and 0.1M AA, respectively. Fig.8c shows a smoother film adsorbed on the alloy surface for 0.1M AA than that formed on 0.01Mconcentration (Fig. 8b). Also the two are much better than the blank shown in Fig.8a

3.3.Adsorption studies and inhibition mechanism

The primary step in the action of inhibitors in solution is generally agreed to be adsorption on the metal or alloy surface. This involves the assumption that the corrosion reactions are prevented from occurring over the area (or active sites) of the metal or alloy surface covered by adsorbed inhibitor species, whereas these corrosion reaction occurred normally on the inhibitor free area [32]. Accordingly, the fraction of surface covered with inhibitor species (θ=IE%100) can followed as a function of inhibitor concentration and solution temperature. The surface coverage (θ) data are very useful while discussing the adsorption characteristics. When the fraction of surface covered is determined as a function of the concentration at constant temperature, adsorption isotherm could be evaluated at equilibrium condition. The dependence of the fraction of the surface covered θ on the concentration C of the inhibitor was tested graphically by fitting it to Langmuir's isotherm, which assumes that the solid surface contains a fixed number of adsorption sites and each site holds one adsorbed species.

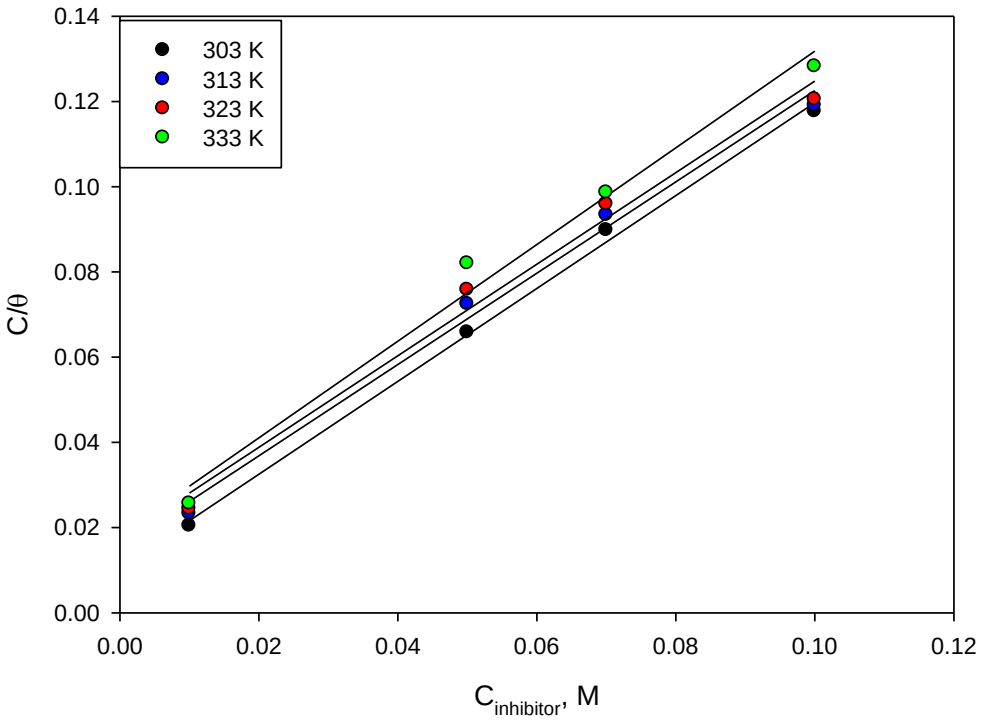

Figure 9. Langmuir adsorption isotherm model for low carbon steel in produced water (blank) containing AAatdifferent temperatures

Fig.9 shows the linear plots for C/θ versus C at different temperatures. The values of K and the correlation coefficient of Langmuir's isotherm are tabulated in Table 3, suggestion that the adsorption obeys the Langmuir's isotherm [33]:

$$\frac{C}{\theta}=\frac{1}{K}+C \qquad (3)$$

where C is the equilibrium inhibitor concentration, K adsorptive equilibrium constant, representing the degree of adsorption (i.e., the higher the value of K indicates that the inhibitor is strongly adsorbed on the metal surface), which obtained from the reciprocal of intercept of Langmuir plot line, and the slop of this line is near unity meaning that each inhibitor molecules occupies one active site on the metal surface.

The standard adsorption free energy ΔG°_{ads} was calculated using the following equation[34]:

$$K=\frac{1}{\mathrm{C}_{\mathrm{H_2O}}}\exp\left(-\frac{\Delta G^{\circ}_{ads}}{RT}\right) \qquad (4)$$

where $\mathrm{C}_{\mathrm{H_2O}}$ are the concentration of water(the same as that of inhibitor concentration) in solution expressed in mol/l, R is gas constant, and T absolute temperature. The average value of standard adsorption free energy ΔG°_{ads} was -17.3 kJ/mol.

Table 4. The estimated values of R_L for different concentrations of AA at different temperatures.

Temp. (K)	Conc. (M)	R_L
303	0.10	0.1500
	0.07	0.2400
	0.05	0.2200
	0.01	0.5100
313	0.10	0.1500
	0.07	0.1900
	0.05	0.2400
	0.01	0.3900
323	0.10	0.0700
	0.07	0.0900
	0.05	0.1100
	0.01	0.1700
333	0.10	0.0200
	0.07	0.0300
	0.05	0.0310
	0.01	0.0600

The negative value of ΔG°_{ads} ensure the spontaneity of the adsorption process and stability of the adsorbed layer on the metal surface. Generally, value of ΔG°_{ads} up to -20 kJ mol^{-1} is consistent with electrostatic interaction between the charged molecules and the charged metal (physisorption) while those around -40 kJ mol^{-1} or higher are associated with chemisorptions as a result of sharing or transfer

of electrons from the molecules to the metal surface to form a coordinate type of bond [35]. While other researchers suggested that the range of ΔG°_{ads} of chemical adsorption processes for inhibitor in aqueous media lies between -21 and -42 kJ mol^{-1} [36]. Therefore, for present work the values of ΔG°_{ads} has been considered within the range of physical adsorption.

Moreover, the essential characteristic Langmuir isotherm can be expressed in term of a dimensionless separation factor, R_L [36] , which describe the type of isotherm and defined by:

$$R_L = \frac{1}{1+KC} \qquad (5)$$

The smaller R_L value indicates a highly favorable adsorption. If R_L>1 unfavorable, R_L= 1 linear, 0 <R_L <1 favorable, and if R_L=0 irreversible.

Table 4 gives the estimated values of R_L for ascorbic acid at different concentrations . It was found that all R_L values are less than unity conforming that the adsorption processes is favorable.

Recent researches have looked into the action of an adsorptive inhibitor from a purely mechanistic kinetic point of view [37]. This relation can be expressed as follow:

$$\log \frac{\theta}{1-\theta} = \log K' + y \log C \qquad (6)$$

A plot of $\log \frac{\theta}{1-\theta}$ versus log C gives a straight line of slop y and intercept of $\log K'$, as shown in Fig. 10.

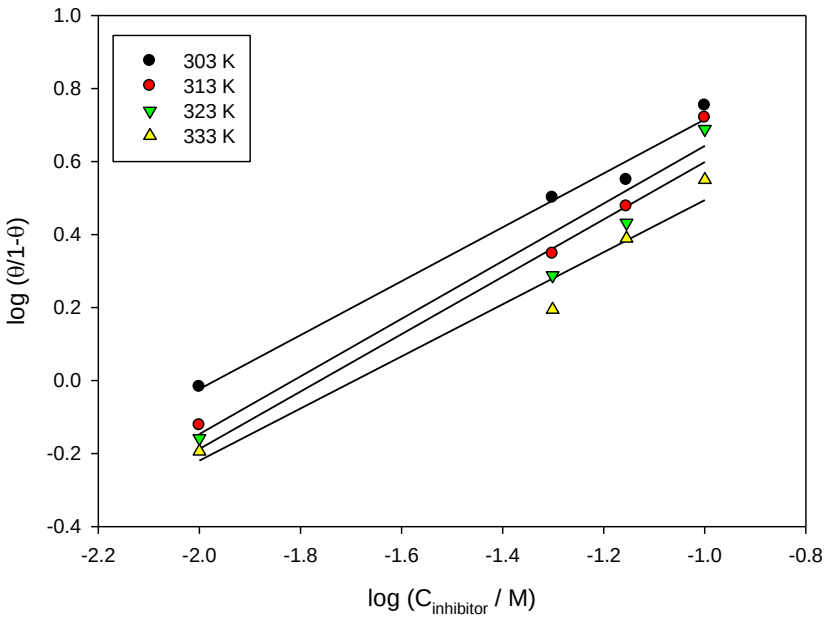

Figure 10. Kinetic-Thermodynamic adsorption isotherm model for low carbon steel in produced water (blank) containing AA at different temperatures

Equilibrium constant corresponding to adsorption isotherm is given by, $K = K'^{\left(\frac{1}{y}\right)}$. where y is the number of inhibitor molecules occupying one active site. Values of y >1 implies the formation of

multilayer of inhibitor on the surface of metal. Values of y <1 mean a given inhibitor molecules will occupy more than one active site. The behavior of equilibrium constants obtained from Langmuir model was similar to the

values which obtained by kinetic–thermodynamic model. Also the values of y were lower than unity indicating the formation of monolayer on the metal surface which agree the assumptions of Langmuir adsorption isotherm. According to langmuir and Kinetic-thermodynamic models the value of the binding constant K decreases with increasing the temperature. This clearly indicates that the strength of electrical interactions by adsorbing molecules and surface of the metal decreases with temperatures.

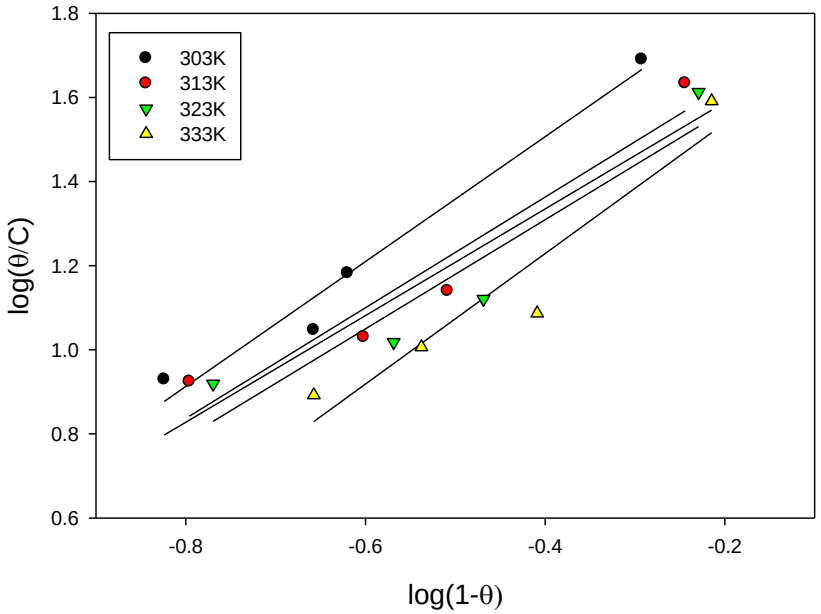

Figure 11. Flory-Huggin adsorption isotherm model for low carbon steel in produced water (blank) containing AA at different temperatures

The results in Table 3 show that on increasing the temperature from 303-323K the number of active sites occupied by one molecule of inhibitor, 1/y, decreases slightly from 1.35 to 1.27 and at 333K it records 1.4. This suggests that most of the inhibitors are adsorbed through more than one active centers and occupy more than one active sites on steel surface (1/y > 1). It is rightful to note that the values of 1/y(x), K and ΔG°_{ads} obtained from kinetic-thermodynamic model are in good agreement with the values calculated from Flory-Huggins isotherm and are matching the order of changing the protection efficiency as reported previously.

Figure 11 gives the results of Flory-Huggins adsorption isotherm for the corrosion inhibition data of ascorbic acid on low carbon steel. Very satisfactory fit is obtained for data of all compounds employed. The slope of the straight lines is **x**, assuming that x = 1/y, and the intercept is log x K according to the following relation[38]:

$$\log\frac{\theta}{C} = \log xK - x\log(1-\theta) \qquad (7)$$

Table 3 gives the adsorption parameters obtained from Kinetic-thermodynamic model and Flory-Huggins adsorption isotherm.

Experimental results obtained were further fitted into Dubinin–Radushkevich isotherm model (DRIM). This model was initially used to distinguish between physical and chemical adsorption for removal of some pollutants from aqueous solutions by adsorption on various adsorbents [39]. Recently, Solomon et al [40] has applied this model in explaining the mechanism of adsorption of corrosion inhibitor onto a metal surface in acidic medium. The equation for the isotherm model can be expressed as:

$$\ln\theta = \ln\theta_{max} - a\partial^2 \quad (8)$$

where θ_{max} is the maximum surface coverage and δ (kJ mol^{-1}) is a constant related to the energy of adsorption and can be correlated as:

$$\partial = RT \ln\left[1 + \frac{1}{C_{inh}}\right] \quad (9)$$

where C_{inh} is the concentration of the inhibitor, 'a' is mean adsorption energy (mol^2 kJ^{-2}),

E_t, which is the transfer energy of 1 mol of adsorbate from infinity (bulk solution) to the surface of the adsorbent (kJ mol^{-1}).

$$E_T = \frac{1}{\sqrt{2a}} \quad (10)$$

Values of E_T less than 8 kJ/mol indicate physical adsorption [41]. The relationship between ln θ and δ^2 for the data obtained for the low carbon steel in produced water at 303-333 K are shown in Figs.12.

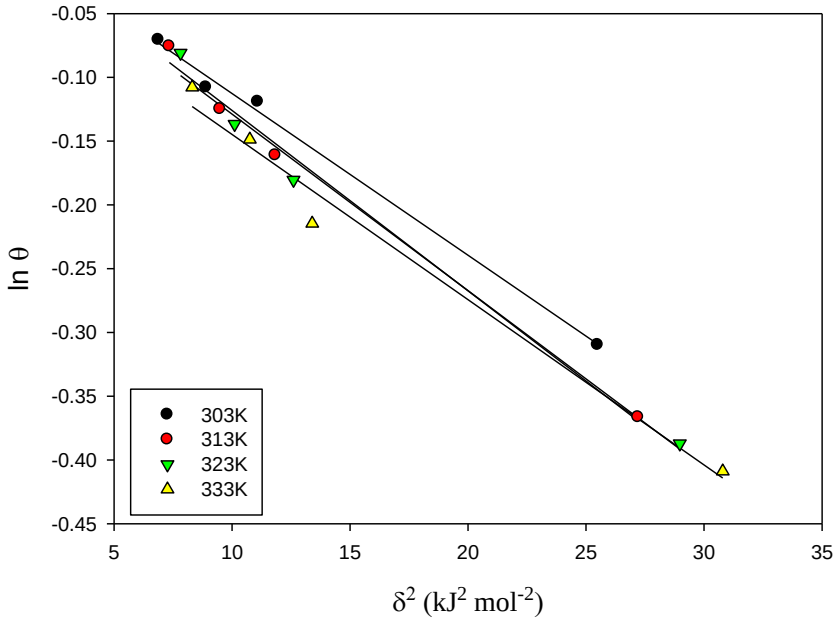

Figure 12. Dubinin–Radushkevich adsorption isotherm model for low carbon steel in produced water (blank) containing AA at different temperatures

The corresponding parameters from the regression analysis are listed in Table 3. It is clear from the table that the numerical values of E_T are less than 8 kJ/mol and reflect physical adsorption mechanism. The values of θ_{max} (maximum surface coverage) are close to 1 indicating good surface coverage by ascorbic acid even at 333K.

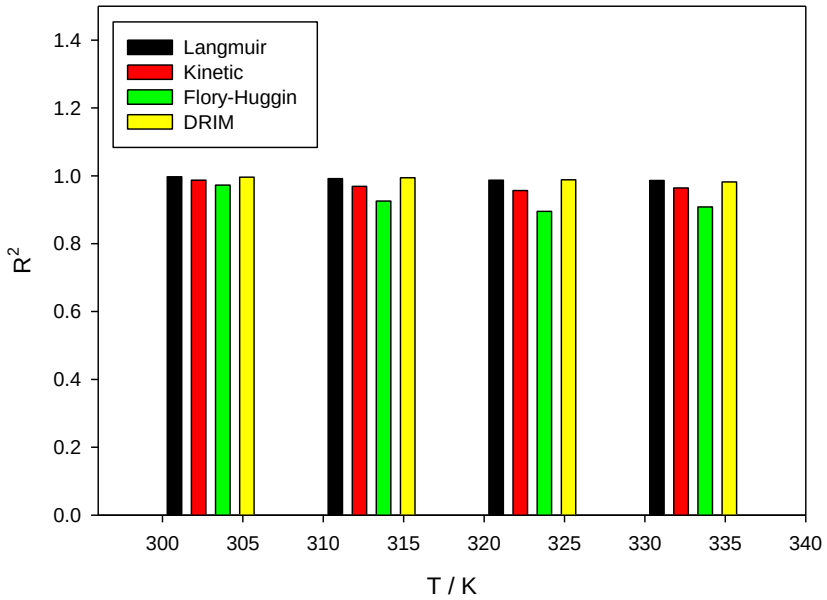

Figure 13. Relation between the correlation coefficient (R^2) and temperature for the different adsorption isotherm models applied for AA inhibitor

Fig.13 shows the relation between the correlation coefficient (R^2) and temperature for the different adsorption isotherm models applied for AA inhibitor. It is seen from the figure that all the adsorption isotherm models used are fitted well at studied temperatures.

3.4.Standard thermodynamic parameters

Thermodynamic parameters play an important role in understanding inhibitive mechanism. The enthalpy (ΔH) and entropy, (ΔS) were obtained from the Eyring transition state equation:

$$\ln \rho = \ln \frac{RT}{Nh} + \frac{\Delta S}{R} - \frac{\Delta H}{RT} \qquad (11)$$

where ρ is the corrosion rate (g cm^{-2} day^{-1}), h is the Planck's constant (6.626176 x 10^{-34} Js) and N is the Avogadro's number (6.02252 x 10^{23} mol^{-1}).

Fig. 14 shows the plot of ln ρ /T versus 1/T for low carbon steel corrosion in produced water in the absence and presence of different concentrations of AA. Straight lines were obtained with a slope of (-ΔH/R) and an intercept of [ln (R/Nh) + (ΔS/R)] from which the values of ΔH and ΔS respectively were calculated and listed in Table 5.

Table 5. Calculated values of thermodynamic parameters for low carbon steel in produced water in the absence and presence of different concentrations of AA

Conc. (M)	ΔH (kJ mol^{-1})	E_a (kJ mol^{-1})	ΔS (J mol^{-1})
0.10	-27.1	29.7	-140.6
0.07	-24.5	27.1	-145.6
0.05	-23.9	26.5	-144.5
0.01	-24.5	27.2	-139.8
0.00	-37.8	40.4	-91.3

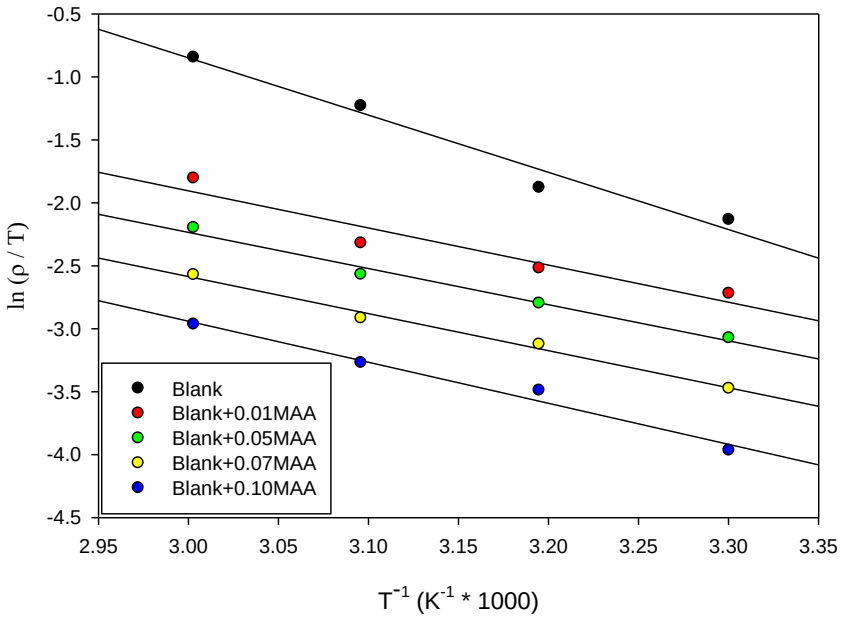

Figure 14. Plot of ln ρ /T versus 1/T for low carbon steel corrosion in produced water in the absence and presence of different concentrations of AA

Generally, an exothermic process signifies either physical adsorption or chemical adsorption. The heat of physical adsorption is relatively low, on the order of 4 – 41 kJ mol^{-1}, whereas that of chemisorption is much higher, of a magnitude of 100–500 kJ mol^{-1} [42]. The *ΔH* value for low carbon steel in produced water (blank) is -37.8 kJ mol^{-1} and addition of AA shifted *ΔH* values to less negative values indicating that adsorption of AA on the steel surface is favored at high temperatures which also indicates that inhibition efficiency (IE%) increases with increasing the temperature. Also, this indicated that the adsorption of AA followed both physical as well as chemical adsorption mechanism.

The values of Δ*S* are negative both in the uninhibited and inhibited systems as well the absolute *ΔS* values increases on increasing AA concentration. The value of Δ*S* obtained for steel in produced water(blank) is -91.3 J mol^{-1} K^{-1} and addition of AA shifted Δ*S* value to more negative values (Table 5). This implies that a greater degree of orderliness appears during addition of AA.

5. CONCLUSION

Ascorbic acid (AA) has proved to be a good corrosion inhibitor for low carbon steel in produced water. Inhibition efficiencies were found to increase with increasing both of the inhibitor concentration and temperature range 303–333K. The concentration of 0.1M AA required to achieve maximum corrosion inhibition efficiency (88%) at 333K. Potentiodynamic polarization results indicate that AA acted as a anodic - type inhibitor. The percentage inhibition efficiencies obtained from Tafel polarization and electrochemical impedance spectroscopy measurements show good agreement with each other. The inhibition of low carbon steel in produced water was found to obey Langmuir, Kinetic-thermodynamic,Flory-Huggins and Dubinin–Radushkevich adsorption isotherms. The thermodynamic values obtained from this study indicate that the adsorption of AA on low carbon steel followed both physical as well as chemical adsorption mechanism.

References

1. M.Ayazi, S.Merfindreski, A.Moghadam,M.Monavarian, *Petrolum&coal*, 48(2)(2006) 6
2. K.D.Efird, R.J.Jasimski, *Corrosion*, 615(1989) 24
3. D.B.Lebsack, D.Hawm, *Mater. Perform.*, 37(1998) 24
4. B.G.Balashov, L.T.Shichalina, *Prot. Me*t., 24(1989)758
5. V.F.Voloshin, O.P.Golosova, L.A.Mazalevskaya, V.S.Bakumenko, A.K.Sheinkman, *Prot. Met*., 24(1986) 685
6. A.M.Fekry, M.A.Ameer, *Int. J. Hydrogen Energy*, 36(2011)11207
7. A.Popova, M.Christov, *Corros. Sci*., 48(2006)3208
8. M.A.Ameer, A.M.Fekry, *Int. J. Hydrogen Energy*, 35(2010)11387
9. A. S. Fouda, A. Hamdy Badr, *African. Pure Appl. Chem.*, 7(10)(2013) 350
10. R.J.Chin, K. Nobe, *Electrochem. Soc.*, 118(1971)545
11. R.Agrawal, T.Namboodhiri, *Appl. Electrochem*., 22(1992)383
12. N.Elkadar, K.Nobe, *Corrosion*, 32(1976)128
13. B.Mernari, H.Elattari, M.Traisnel, F.Bentiss, M.Lagrenee, *Corros. Sci.*, 40(1998)391
14. F.Bentiss, M. Lagrenee, M. Traisnel, J. Hornez, *Corros. Sci.*, 41(1999)789
15. E.S.Ferreira, C.Giacomelli, A.Spinelli, *Mat. Chem.Phys*., 83(2004) 129
16. R.S.Goncalves, L.D.Mello, *Corros. Sci*., 43(2001)457.
17. I.Sekine, Y.Nakahata, H.Tanabe, *Corros. Sci*., 28(1998)987
18. L.Li, A.A.Sagüés, *Corrosion*, 58(2002)305
19. L.Valek, S. Martinez, M.Serdar, I.Stipanovic, *Chem. Biochem. Eng*., 21(2007) 65.
20. P.Morales-Gil, G.Negron-Silva, M.Romero-Romo, C.Angeles-Chavez, M.Palomar-Pardave, *Electrochim. Acta.*, 49(2004)4733
21. A.M.Fekry, M.A.Ameer, *Int. J. Hydrogen Energy*, 35(2010)7641
22. A.A. Ghoneim, A.M. Fekry, M.A. Ameer, *Electrochim. Acta.*, 55(2010)6028
23. P.Morales-Gil, G.Negro´ n-Silva, M. Romero-Romo, C.A ngeles-Chavez, M. Palomar-Pardave, *Electrochim. Acta.* 49 (2004) 4733
24. M.A.Ameer, A.M.Fekry, A.A. Ghoneim, F.A.Attaby, *Int. J. Electrochem. Sci.*, 5(2010)1847
25. I.Sekine, Y.Nakahata , H.Tanabe, *Corros. Sci*., 28(1998)987
26. Y.Nishikawa, T.Kurata, *Biosci. Biotechnol. Biochem.*, 64(2000)476
27. P.K.South, D.D.Miller, *Food Chem.*, 63(1998)167.
28. K.Gamal, K.Gomma, H.Mostafa, H.Wahdan, *Mat .Chem. Phys*., 39(1995)209
29. M.A.Ameer, A.M.Fekry, *Int. J. Hydrogen Energy*., 35(2010)11387

30. L.NnannaL, B.Onwuagba, I.Mejeha, K.Okeoma, *African. Pure Appl. Chem*., 4(1)(2007)011
31. N.Eddy, E.Ebenso, *African. Pure Appl .Chem*. 2(6)(2008)46
32. L.L.Shereir, Corrosion, vol. 2, second ed., Newnes-Butterworths, London 1977
33. R.Alberty, R. Silbey, Physical Chemistry, second edition, Pub. Wiley & Sons,1997, USA, p. 845
34. M.A.Ameer, A.M.Fekry, *Progress in Organic Coatings*., 71(2011)343
35. E.Umoren, E.Ebenso, *Mater. Chem. Phys*., 106(2007)393
36. A.A.Khadom, A.S.Yaro, A.S.AlTaie, A.A.Kadum, *Portug. Electrochim. Acta*, 27(6)(2009)699
37. S.K.Shukla, M.A.Quraishi, R.Prakash, *Corros. Sci.*, 50(2008)2867
38. H.Dhar, B.Conway, K.Joshi, *Electrochim. Acta*., 18(1973) 789
39. I.D.Mall, V.C.Srivastava, N.K.Agarwal, I.M.Mishra, *Colloids Surf. A: Physicochem. Eng. Asp.*, 264(2005) 17
40. M.M.Solomon, S.A. Umoren, I.I.Udosoro, A.P.Udoh, *Corros. Sci*., 52(2010)1317.
41. E.A.Noor, *Appl. Electrochem*., 39(2009)1465
42. M.A.Amin, K.F.Khaled, Q.Mohsen, H.A.Arida, *Corros. Sci*., 52(2010)1684